

Research paper

Drug release mechanism of paclitaxel from a chitosan–lipid implant system: Effect of swelling, degradation and morphology

Patrick Lim Soo^a, Jaepyoung Cho^a, Justin Grant^a, Emmanuel Ho^a,
Micheline Piquette-Miller^a, Christine Allen^{a,b,*}

^a Department of Pharmaceutical Sciences, University of Toronto, ON Canada

^b Department of Chemistry and Chemical Engineering & Applied Chemistry, University of Toronto, ON Canada

Received 12 June 2007; accepted in revised form 8 November 2007

Available online 17 November 2007

Abstract

Localized and sustained delivery of anti-cancer agents to the tumor site has great potential for the treatment of solid tumors. A chitosan–egg phosphatidylcholine (chitosan–ePC) implant system containing PLA-*b*-PEG/PLA nanoparticles has been developed for the delivery of paclitaxel to treat ovarian cancer. Production of volumes of ascites fluid in the peritoneal cavity is a physical manifestation of ovarian cancer. *In vitro* release studies of paclitaxel from the implant were conducted in various fluids including human ascites fluid. A strong correlation ($r^2 = 0.977$) was found between the release of paclitaxel in ascites fluid and PBS containing lysozyme (pH 7.4) at 37 °C. The drug release mechanism for this system was proposed based on swelling, degradation and morphology data. In addition, *in vitro* release of paclitaxel was found to be a good indicator of the *in vivo* release profile (correlation between release rates: $r^2 = 0.965$). Release of paclitaxel was found to be sustained over a four-week period following implantation of the chitosan–ePC system into the peritoneal cavity of healthy Balb/C mice. Also, the concentrations of paclitaxel in both plasma and tissues (e.g. liver, kidney and small intestine) were found to be relatively constant.

© 2007 Elsevier B.V. All rights reserved.

Keywords: Drug release; Polymer–lipid implant; Drug delivery; Paclitaxel; Ascites fluid; Ovarian cancer

1. Introduction

In 2006, an estimated 20,000 new cases of ovarian cancer were diagnosed in the United States [1]. Ovarian cancer causes more deaths than any other cancer of the female reproductive system [2]. The removal of the cancerous mass via surgery in combination with chemotherapy (i.e. paclitaxel and cisplatin/carboplatin) is currently the gold standard treatment for this cancer [3]. However, despite advances in both surgery and chemotherapy, the survival

rate for women with advanced ovarian cancer has not changed over the last four decades [4].

Recently, the National Cancer Institute (U.S.A.) made the recommendation that combinations of intravenous (IV) and intraperitoneal (IP) chemotherapy should be used for the treatment of advanced ovarian cancer (Stage III) [5]. Patients receiving this treatment regimen were reported to have an improvement in their overall survival by about 16 months, in comparison to patients who only received IV chemotherapy [6]. IP administration of chemotherapy can provide an opportunity to directly expose the tumor site to higher concentrations of drug. Paclitaxel is ideal for IP administration due to its complex structure and high molecular weight which are both properties that are known to favor retention in the peritoneal cavity [7]. To this point, clinical IP administration of paclitaxel has included a bolus dose of the drug in the commercially available formulation

* Corresponding author. Department of Pharmaceutical Sciences, Leslie Dan Faculty of Pharmacy, University of Toronto, 144 College St., Toronto, ON Canada M5S 3M2. Tel.: +1 416 946 8594; fax: +1 416 978-8511.

E-mail address: cj.allen@utoronto.ca (P. Lim Soo).

Taxol[®] (i.e. Cremophor EL and absolute ethanol (50/50)). However, sustained IP administration of this drug, which could be achieved using an advanced delivery system, may be advantageous since its cytotoxic effect is dependent on the duration of cell exposure [8].

To date, several depot systems have been designed for local delivery of paclitaxel [9–12]. For example, Harper et al. developed poly(lactide-co-ethylphosphate) microspheres containing paclitaxel (PACLIMER[®]) for treatment of non-small cell lung cancer [9]. Jackson et al. studied the use of an ABA triblock copolymer (i.e. poly(D,L-lactide-co-caprolactone)-*block*-polyethylene glycol-*block*-poly(D,L-lactide-co-caprolactone)) blended with methoxypolyethylene glycol to form a paste for the local delivery of paclitaxel [11]. Also, an injectable system (OncoGel) formed from a triblock copolymer of poly(lactide-co-glycolide)(PLGA) and PEG recently entered Phase I trials for local delivery of paclitaxel to various solid tumor sites (e.g. breast, non-Hodgkins lymphoma and lung) [12]. Therefore, to this point most of the depot systems for paclitaxel consist of a matrix formed from polyesters which are known to illicit fibrous capsid formation [13,14].

In contrast, our group has evaluated an implantable delivery system formed from chitosan and egg phosphatidylcholine (ePC) for sustained delivery of paclitaxel [15–19]. In this system paclitaxel is loaded into biocompatible [poly-D,L-lactide (PLA) and poly(lactide)-*block*-poly(ethylene glycol) (PLA-*b*-PEG)] nanoparticles that are dispersed in a polymer-lipid matrix. This chitosan-ePC implant system has been shown to be biocompatible both *in vitro* in SKOV-3 cells, an ovarian carcinoma cell line and *in vivo* in CD-1 mice [15]. Importantly, fibrous encapsulation of the implant was not detected in mice 2–4 weeks after surgical implantation [15]. As well, the chitosan-ePC implant system was found to increase the maximum tolerated dose of paclitaxel and enhance anti-tumor efficacy in a human tumor xenograft model of ovarian cancer, in comparison to a commercial paclitaxel formulation (Taxol[®], Bristol-Myers Squibb) [19]. Furthermore, the development of multidrug resistance was found to be attenuated in mice treated with the PTX-chitosan-ePc formulation [17].

One of the major issues concerning implantable drug delivery systems is the influence of the local environment on stability of the drug and the system as well as the drug release. Ascites fluid can be caused by intra-abdominal tumors [20] and tends to build up in the peritoneal cavity of individuals afflicted with ovarian cancer. The pH typically ranges from 7.4 to 7.8 and the fluid is composed of various proteins such as serum albumin, and glucose [21]. Due to the large volumes of ascites that can be produced in the peritoneal cavity of patients, the present study evaluated the release profile of paclitaxel and physico-chemical characteristics of the chitosan-ePC implant in human ascites fluid. Data obtained from the characterization of the swelling and degradation profiles as well as the time-dependent morphology of the implant were taken together to elucidate the mechanism of drug release. In addition, the

in vivo release and biodistribution profile of paclitaxel in plasma and various tissues (e.g. heart, liver, kidney and small intestine) was evaluated following IP implantation of the chitosan-ePC implant in healthy Balb/c mice.

2. Materials and methods

2.1. Materials

Paclitaxel was purchased from PolyMed Therapeutics (Houston, Texas, USA). Colchicine (internal standard), HPLC grade acetonitrile and water, poly-(D,L-lactide) (MW 75,000–125,000), crude ePC (purity: at least >60% phosphatidylcholine), ethyl acetate (urethane grade) and lysozyme from chicken egg white were obtained from Sigma-Aldrich (Oakville, ON, Canada). Chitosan (medium molecular weight, MW 400,000 and *ca.* 85% degree of deacetylation) was purchased from Fluka BioChemika (Buchs, Switzerland). Docetaxel (internal standard) was obtained from Sai Life Sciences (Hyderabad, India). 100% ethanol was purchased from Commercial Alcohols Inc. (Brampton, ON, Canada). The PLA₄₁₀₀-*b*-PEG₅₀₀₀ copolymer (polydispersity = 1.07) was synthesized using an established method [16].

2.2. Preparation of PLA-PEG/PLA nanoparticles and preparation of chitosan-ePC implants containing paclitaxel

The PLA-*b*-PEG/PLA nanoparticles containing paclitaxel (100 mg; 1:5 drug: polymer ratio (wt/wt))[16] were prepared using an emulsification-diffusion method that has been described in detail previously [22]. The method for preparation of the chitosan-ePC implant has also been described elsewhere [15,16]. Briefly, a 2% (wt/wt) chitosan solution containing 1% (v/v) acetic acid was prepared in MilliQ water (18.2 MΩ cm, 20 mL). EPC in ethanol was homogenized (Polytron[®] PT-MR 3100, Kinematica AG, Switzerland) with 15 mL of chitosan (i.e. 0.8:1 ePC: chitosan (wt/wt)) and PLA/PLA-*b*-PEG nanoparticles in water. The implant was transferred to a Teflon coated dish and allowed to dry in a desiccator for 7 days at room temperature. The drug to material ratio was 1:8 (wt/wt) and the paclitaxel drug loading efficiency was greater than 90% as measured by HPLC analysis.

2.3. *In vitro* drug release profile and *in vitro* drug stability

Collection of ascites fluid from ovarian cancer patients was approved by the Research Ethics Board of the University Health Network and University of Toronto in collaboration with Dr. Amit Oza and Dr. Alice Newman (Princess Margaret Hospital, Toronto, ON, Canada). The ascites fluid was obtained and pooled from patients who had not received anti-cancer drug therapies for at least five weeks prior to collection. The pH of ascites fluid was approximately 7.7. The lysozyme activity of the ascites fluid was quantified using an EnzChek[®] lysozyme assay

kit (Molecular Probes, Inc., Eugene, OR, USA) [23] while the protein content was determined using a Bradford assay (Bio-Rad Laboratories, Hercules, CA, USA) [24].

The chitosan–ePC containing paclitaxel implants were cut into square pieces (10 × 10 mm, 1 mm thickness) with weights that ranged from 10 to 15 mg. Each implant was placed into a scintillation vial (total volume = 5 mL) and drug release measured under the following conditions ($n = 3$): 0.01 M Phosphate Buffer Saline (PBS) at room temperature (25 °C), 0.01 M PBS at physiological temperature (37 °C), 0.01 M PBS containing 2 mg/mL of lysozyme (pH 7.4) at 37 °C (referred to as PBS lysozyme henceforth) and human ascites fluid at 37 °C. A similar release method was previously used [16]. Briefly, at specific time points, 2 mL of solution was removed from the beaker and immediately replaced with 2 mL of the corresponding solution. The samples were analyzed by HPLC. In addition, HPLC was used to test the stability of the drug in both ascites fluid and PBS lysozyme.

2.4. Swelling and degree of erosion (degradation) of chitosan–ePC implant

Square sized implants (10 × 10 mm, 1 mm thickness) ranging from 10 to 15 mg were incubated at 37 °C with 5 mL of human ascites fluid and for comparison, PBS lysozyme. At specific time points, the implants were removed and quickly rinsed with MilliQ water. The implants were then blotted dry and the initial weight (swollen weight, W_s) was recorded. The implants were dried in an incubator (37 °C) for 24 h and re-weighed (dried weight, W_d). The implants remained intact during the process and no macroscopic pores were visible. Also the geometric shape of the implants remained the same. The degree of swelling was calculated using the following equation [25]:

$$\text{Degree of swelling}(\%) = \frac{W_s - W_d}{W_d} \times 100 \quad (1)$$

The degree of erosion was calculated using the following equation [26] as follows:

$$D_E = 1 - W_R = 1 - e^{-kt} \quad (2)$$

where D_E is the degree of erosion and k is the kinetic rate constant. W_R is the relative weight ratio that was determined experimentally by measurement of the weight of the implant before ($W_d(0)$) and after ($W_d(t)$) drug release at an arbitrary time (t):

$$W_R = \frac{W_d(t)}{W_d(0)} \quad (3)$$

A four-parameter exponential decay equation was used to fit the plot of W_R versus time:

$$W_R = A \exp(-Bt) + C \exp(-Dt) \quad (4)$$

Table 1

The fitting parameters refer to Eq. (4) employed for determination of the time-dependent degree of erosion of the implant system in PBS lysozyme and ascites fluid at 37 °C

Release solution	<i>A</i>	<i>B</i>	<i>C</i>	<i>D</i>
PBS lysozyme	0.19	0.15	0.8	3.5×10^{-3}
Ascites fluid	0.19	1.11	0.8	3.4×10^{-3}

where A , B , C and D represent fitting parameters that are shown in Table 1.

2.5. In vivo studies with the chitosan–ePC implant

In vivo studies were performed in healthy 10-week-old female Balb/c mice (average weight: 21 g) (Charles River, St. Constant, QC, Canada) in accordance with the guidelines from the Canadian Council on Animal Care. Chitosan–ePC implants (drug-free and paclitaxel-containing) were cut into squares (10 × 10 mm, 1 mm thickness) with an average weight of 12 mg. Implants were sterilized under UV light using the Sterilizer T209 (Intercosmetics, Mississauga, ON, Canada) for 3 h and in 80% ethanol prior to implantation. Animals were anesthetized with isoflurane and a one cm incision was made in the left lower quadrant of the abdomen. Sterilized drug-free or paclitaxel-containing chitosan–ePC implants were inserted into the peritoneal cavity and the incision site was sutured. The mice were weighed and observed weekly for signs of distress (e.g. weight loss, colour, lethargy).

At specific time points (one, two, three or four weeks following implantation), blood was withdrawn from the mice via cardiac puncture, the mice ($n = 3$ per time point) were sacrificed and the implant was removed. The blood was centrifuged at 5000 rpm for ten minutes at 4 °C and the supernatant (i.e. plasma) was collected and stored at –80 °C.

In order to extract the paclitaxel from the implant, it was placed in dichloromethane (5 mL) and stirred for a period of 48 h. The implant was then removed and the solvent was dried off under nitrogen. The dried paclitaxel was reconstituted in acetonitrile (3 mL) and an aliquot (20 µL) was taken for HPLC analysis. The extraction efficiency was greater than 90% using this method (i.e. for paclitaxel concentrations ranging from 18 to 31 µg/mL).

2.6. Scanning electron microscopy

Scanning electron microscopy (SEM) of the chitosan–ePC implants, following removal from the peritoneal cavity of Balb/c mice, was performed using a Hitachi S-570 (Hitachi, Tokyo, Japan) operating under vacuum at a voltage of 15 kV. SEM samples were prepared using gold sputter coating with a SC7640 High Resolution Coater (Quorum Technologies, Newhaven, UK). Measurements were made using the Sigma Scan Pro software (Jandel Scientific,

California, USA) to determine the average surface area (SA) of pores (which were assumed to be spherical) in the implants. The equation used to calculate the surface area of the pores was $SA = 4\pi r^2$.

2.7. HPLC analysis and extraction method for plasma and tissues

The HPLC system includes an Agilent Series 1100 (Mississauga, ON, Canada) equipped with a quaternary pump and autosampler, Waters Dual Absorbance Detector 2487 (Milford, MA, USA) and Agilent software. The HPLC system was equipped with a 4.6 mm \times 250 mm column and a 3.9 \times 20 mm guard column (Waters XTerra MS C₁₈ 5 μ m). The wavelength of detection for paclitaxel was 227 nm. For the *in vitro* analysis, the mobile phase used was 50% acetonitrile and 50% water. A 30 min isocratic method was used at a flow rate of 1 mL/min with an injection volume of 20 μ L. In the case of the *in vivo* analysis, the mobile phase used was acetonitrile and 0.01 M PBS (pH 10). For the first 10 min, 40% acetonitrile and 60% PBS were used. The mobile phase was then increased over 1 min to 45% acetonitrile and held for 29 min at a flow rate of 1 mL/min. Colchicine and docetaxel were used as internal standards in the HPLC analysis for the *in vitro* and *in vivo* studies, respectively.

For the extraction of drug from plasma, a plasma sample (100 μ L) was added to a vial containing docetaxel (1 μ g/mL) and the contents were vortexed. Ethyl acetate (5 mL) was then added to extract paclitaxel and the sample was placed on a mechanical shaker for 10 min. The solution was centrifuged (Eppendorf Centrifuge 5804R, Hamburg, Germany) at 4000 rpm for 15 min. The organic layer was transferred to a new vial prior to drying under nitrogen. The sample was then re-suspended in mobile phase and analyzed by HPLC. The extraction efficiency of paclitaxel from plasma was greater than 90% (0.01–1 μ g/mL). For the extraction of drug from tissues, deionized water was added at ratio of 4 mL/g to tissues samples. The tissues were then homogenized (Fisher Model 100 Sonic Dismembrator (Ottawa, ON, Canada)) and added to a vial containing docetaxel (1 μ g/mL). The extraction procedure was then similar to that described above for plasma. The sample was reconstituted with mobile phase and analyzed by HPLC. The extraction efficiency of paclitaxel from tissues was greater than 80% (0.02–1 μ g/mL).

2.8. Statistical analysis

Data were analyzed using an *F*-test with subsequent *T*-tests (equal variance) for comparison between two different groups. For 3 or more different groups, ANOVA was used followed by a Least Significant Differences method. Results were considered statistically significant at $p < 0.05$. All data are presented as mean values with standard error (mean \pm SE).

3. Results and discussion

3.1. *In vitro* drug release

As shown in Fig. 1, the *in vitro* release of paclitaxel from the chitosan–ePC implant was evaluated under various conditions. The paclitaxel was confirmed to be stable for the first 2 months of the release study at 37 °C (data not shown). The cumulative release of drug from the chitosan–ePC implant after 7 days was only $1.0 \pm 0.01\%$ and $1.4 \pm 0.11\%$ in PBS at 25 °C and 37 °C, respectively. This slow release continued for up to 84 days, at which time, the release for PBS was $6.7 \pm 0.09\%$ and $9.4 \pm 0.10\%$ at 25 and 37 °C, respectively. In the presence of lysozyme and ascites fluid, a total of 62% and 69% of paclitaxel (represents a release rate of about 1% per day), respectively, was released over the same period of time (i.e. 84 days). The large difference in release between PBS and PBS lysozyme is due to the presence of the lysozyme which is used to degrade chitosan *in vivo* [16].

An excellent correlation ($r^2 = 0.977$) was obtained between the release profiles for paclitaxel in ascites fluid and PBS lysozyme (Fig. 1 inset). This indicates that the *in vitro* release of drug from the implant in PBS lysozyme provides an accurate prediction of the release in ascites fluid, which is the environment found in the peritoneal cavity of ovarian cancer patients. Importantly, no burst release was observed for the release of paclitaxel from the implant under all incubation conditions. In contrast, Liang et al. observed a 20% burst release of paclitaxel from poly(γ -glutamic acid)-poly(lactide) nanoparticles due to the localization of paclitaxel to the periphery of the nanoparticles [27]. Similarly, vitamin E TPGS-emulsified PLA, PLGA(75:25) and PLGA(50:50) all displayed an initial burst release of

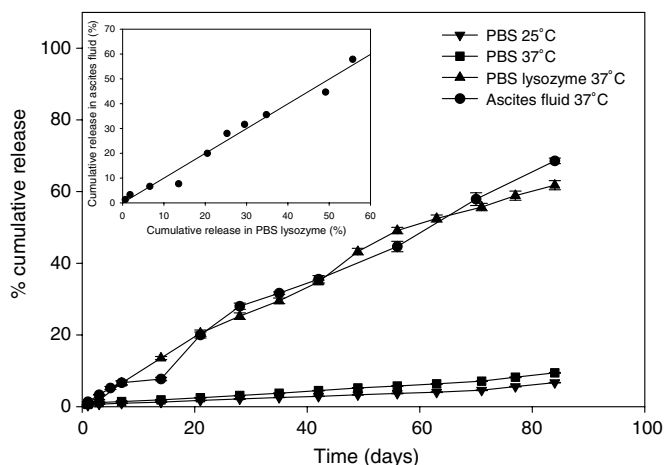


Fig. 1. *In vitro* release of paclitaxel from chitosan–ePC implant under various conditions: PBS at 25 °C (\blacktriangledown) and 37 °C (\blacksquare), PBS lysozyme at 37 °C (\blacktriangle) and human ascites fluid (pH 7.6–7.8) at 37 °C (\bullet). Error bars are expressed as standard error ($n = 3$). Inset: Correlation ($r^2 = 0.977$) between *in vitro* release of paclitaxel from implant in ascites fluid and PBS lysozyme.

paclitaxel with more than 15% of the drug being released after 24 h [28]. Hence, the chitosan–ePC matrix provides a reliable barrier to minimize the burst release of paclitaxel from the nanoparticles [15].

3.2. Fitting of drug release profile from chitosan–ePC implant

The power law has commonly been used to describe the diffusion of solutes through polymers [29]. The equation is as follows:

$$\frac{M_t}{M_\infty} = k_1 t^{n_1} \quad (5)$$

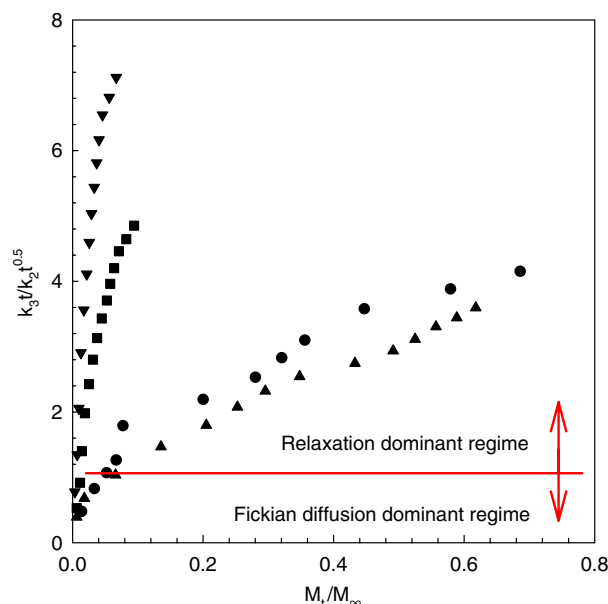
where M_t/M_∞ is the amount of drug released, t is the time of release, k_1 is the kinetic constant and n_1 is the diffusion exponent, which is related to the drug release mechanism [30]. For a thin slab geometry, when $n_1 = 0.5$, this represents a Fickian diffusion mechanism. When $n_1 = 1$, a Case II transport mechanism is operative in which drug release from the slab is zero-order. In the case when n_1 is between 0.5 and 1, the transport is atypical and both Fickian diffusion and Case II transport contribute to the release [31].

Peppas–Sahlin developed a release model [32] which takes into account both Fickian and Case II transport contributions and the equation describing release in this model is as follows:

$$\frac{M_t}{M_\infty} = k_2 t^{n_1} + k_3 t^{2n_1} \quad (6)$$

where k_2 and k_3 are kinetic constants and n_1 is indicative of the type of release mechanism. In Eq. (6), the effect of Fickian diffusion on drug release is represented as $k_2 t^{0.5}$, since $n_1 = 0.5$. The second term ($k_3 t$) is related to Case II transport, since $2n_1 = 1$. When the ratio of both contributions (i.e. $k_3 t/k_2 t^{0.5}$) is greater than 1, the drug release occurs predominantly by macromolecular relaxation. When the ratio is less than 1, the drug release occurs mainly by diffusion.

The drug release of paclitaxel from the chitosan–ePC implant was fit using the power-law equation Eq. (5) and the kinetic constants and the diffusion coefficients are included at the bottom of Fig. 2. The values of n_1 were between 0.5 and 1, which indicates that paclitaxel was released by a combination of Fickian diffusion and Case-II transport processes. In order to decouple these two processes, the release data were fit using the Peppas–Sahlin model as shown in Fig. 2 (i.e. r^2 greater than 0.97 for all conditions). The kinetic constants were used to determine the extent to which macromolecular relaxation contributes to drug release. In PBS lysozyme and ascites from days 0 to 7, the values for the ratio were less than one (i.e. indicative of release by diffusion), while following day 7, they were greater than one. This indicates that during this period (i.e. after 7 days) the main driving force for paclitaxel release was the macromolecular relaxation which occurred within the chitosan–ePC matrix.



T (°C)	Release solution	Power law equation		Peppas–Sahlin	
		k_1	n_1	k_2	k_3
25	PBS ▼	1.2×10^{-3}	0.91	8.0×10^{-4}	6.0×10^{-4}
37	PBS ■	1.4×10^{-3}	0.93	1.6×10^{-3}	9.0×10^{-4}
37	PBS/lysozyme ●	1.5×10^{-2}	0.84	1.5×10^{-2}	6.1×10^{-3}
37	Ascites ▲	1.6×10^{-2}	0.83	1.4×10^{-2}	6.5×10^{-3}

Fig. 2. *In vitro* release of paclitaxel from the chitosan–ePC implant under various conditions fit using the Peppas–Sahlin model Eq. (6). The ratio of the contribution of Case II transport ($k_3 t$) and the contribution of the Fickian processes ($k_2 t^{0.5}$) is plotted as a function of drug release (M_t/M_∞).

3.3. *In vitro* swelling of chitosan–ePC implant and effect of swelling on drug release of paclitaxel

In the case of a biodegradable and expandable implant system, the effect of swelling on the diffusivity of the drug is an important parameter that influences the release profile. The chitosan–ePC implant is a three-dimensional physical network stabilized by intermolecular forces, such as ionic and hydrophobic interactions, between chitosan and ePC [16]. As shown in Fig. 3, the degree of swelling for the chitosan–ePC implants reached relatively constant values following 24 h and was not significantly different in ascites and PBS lysozyme ($p > 0.05$). Therefore, the swelling of the matrix has the most profound influence on drug release within the first 24 h, following this period the system is fully swollen in both ascites and PBS lysozyme. The swelling results obtained for the implant in PBS (data not shown) were in agreement with our previous report (approximately 260%) [16]. In addition, the absorption of water in the implant could have a dilution effect (i.e. decreasing the polymer concentration), thus decreasing the number of entanglements between the macromolecules as well as enhancing the water concentration in the implant [31]. This results in a loosened matrix, which allows a bulky drug like paclitaxel to easily move from the matrix to the aqueous medium. Thus, diffusion of the drug is facilitated in the swollen matrix.

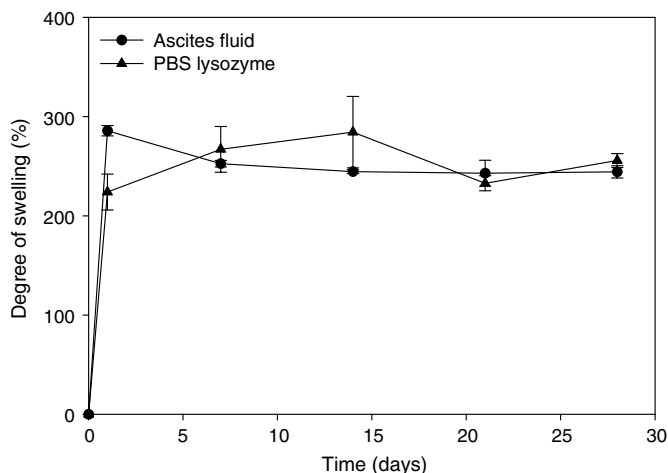


Fig. 3. Degree of swelling of chitosan–ePC implant in PBS lysozyme (\blacktriangle) and ascites fluid (\bullet) at 37 °C. Error bars are expressed as standard error ($n = 3$).

For the release of paclitaxel in the absence of lysozyme, the calculated n_1 values were 0.91 and 0.93 for 25 and 37 °C, respectively (bottom of Fig. 2). These high values for n_1 may be related to increased water availability in the matrix [33]. Water is absorbed by the matrix and destroys intra- and intermolecular hydrogen bonds, resulting in the formation of pores and/or enlargement of current existing pores. Fang et al. observed this effect for the release of drugs ranging in molecular weight (60–236 g/mol) from chitosan/gelatin hybrid membranes [34]. In the swollen implant, water can penetrate the implant through the pores. Thus, the generation of pores and enlargement of the pore size increase the total area available for drug release and decrease the distance required for diffusion of the drug from matrix to aqueous medium. In this way, the drug continues to diffuse through the implant. However, the n_1 values were decreased for the paclitaxel release to 0.84 and 0.83 in PBS lysozyme and ascites fluid, respectively. Xiong et al. suggested that the drug release is mainly controlled by degradation when n_1 values are close to 0.85 [35]. Lysozyme molecules (spherical molecular diameter ~ 3.2 nm) [36] and other enzymes could occupy the water filled pores in order to diffuse through the matrix. Thus, the water availability is lessened with the presence of enzymes in the PBS lysozyme and ascites solutions, in comparison to PBS alone.

3.4. In vitro degradation of chitosan–ePC implant and effect of degree of erosion on drug release of paclitaxel

The degree of erosion for the drug release in PBS lysozyme and ascites fluid was obtained using Eq. (2) as shown in Fig. 4. The degradation profile can be divided into two regions depending on the rate of degradation: region 1 is characterized by a fast rate and region 2 is characterized by a relatively slow rate. The parameters B and D represent the degradation rate as shown in Table 1. Initially, the deg-

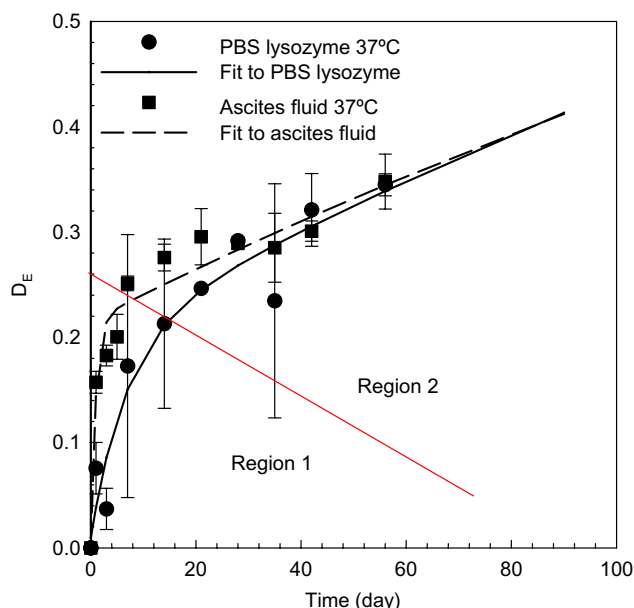


Fig. 4. Degree of erosion (D_E) fit to a four-parameter exponential decay equation: $W_R = A \exp(-Bt) + C \exp(-Dt)$.

radation constant was high (e.g. $B = 1.11 \text{ day}^{-1}$) in ascites fluid compared to PBS lysozyme. However, the rate of degradation of the implant became similar in both solutions over time (i.e. $3.4\text{--}3.5 \times 10^{-3} \text{ day}^{-1}$). Hence, the release of paclitaxel from the implant is influenced not only by swelling, but also by degradation.

Lysozyme has been shown to have enzymatic activity against beta 1–4 glycosidic linkages, which are present in chitosan [37]. The degradation of chitosan–ePC in PBS lysozyme is mainly due to enzymatic hydrolysis [38]. The protein concentration in ascites fluid (i.e. $10.3 \pm 0.13 \text{ g/L}$) was 5 times higher than that in PBS lysozyme (i.e. $2.02 \pm 0.16 \text{ g/L}$); however, the lysozomal activity of ascites was determined to be less (i.e. $136 \pm 6 \text{ U/mL}$) in ascites as compared to the prepared PBS lysozyme ($227 \pm 8 \text{ U/mL}$). It is highly plausible that ascites fluid contains several other proteins or enzymes which contribute to the degradation of chitosan [39]. It should be noted that no significant difference was found between the pH of the PBS lysozyme and ascites fluid solutions over the entire incubation period (i.e. $\text{pH} \cong 7.7 \pm 0.1$).

3.5. Morphology of the chitosan–ePC implant

Scanning electron micrographs were taken of chitosan–ePC implants that had been implanted in the IP cavity of Balb/c mice for 4 weeks as shown in Fig. 5. Following a one week period, the SEM image revealed that there were nanoparticles present at the surface of the film (Fig. 5a). The nanoparticles appeared to be both smooth and spherical. The size of the PLA/PLA-b-PEG nanoparticles ($344 \pm 28 \text{ nm}$) has been reported previously [16]. Nanoparticles can still be seen inside of the pores of the implants in

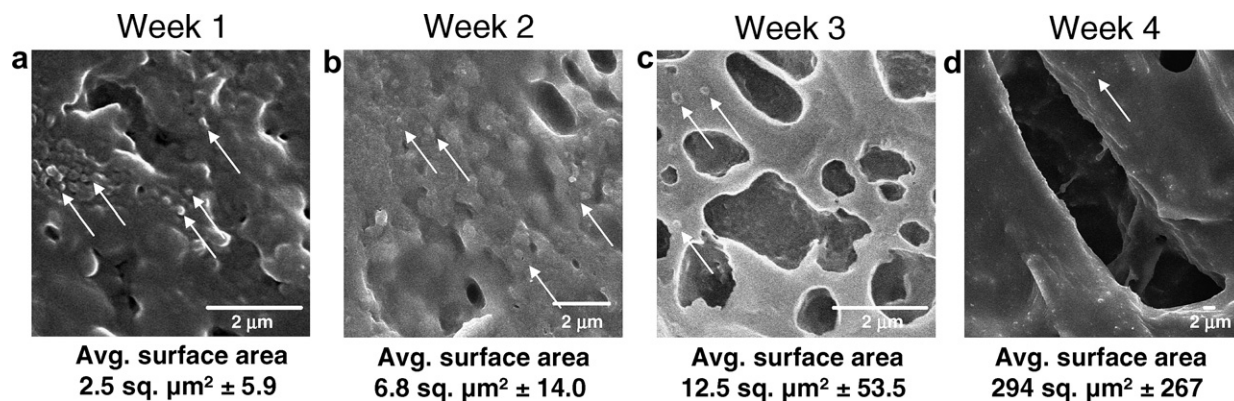


Fig. 5. Scanning electron micrographs of chitosan-ePC implant implanted in Balb/c mice for periods up to 4 weeks. The arrows indicate the PLA-b-PEG/PLA nanoparticles. Error bars for the average surface areas (SA) are expressed as standard error ($n = 140$).

weeks two and three (Fig. 5b and c), although by week four (Fig. 5d), there are fewer nanoparticles present. The degradation of the implant has resulted in the removal of some of the nanoparticles from the matrix. There were very few pores after week 1, however, additional and larger pores appeared in the SEM images as the weeks progressed. The average surface area of the pores was calculated for each week (i.e. Week 1: $2.5 \text{ sq. } \mu\text{m}^2$, Week 2: $6.8 \text{ sq. } \mu\text{m}^2$, Week 3: $12.5 \text{ sq. } \mu\text{m}^2$ and Week 4: $294 \text{ sq. } \mu\text{m}^2$), with the assumption that the pores are spherical in size ($n = 140$).

3.6. Proposed mechanism of drug release from chitosan-ePC implant

Initially, the occurrence of swelling increased the free volume in the chitosan-ePC implant. The absorption of water increased the mobility of the drug molecules via a plasticizing effect, disrupting both intra- and intermolecular hydrogen bonds, resulting in the generation of new pores and/or enlargement of current existing pores. As a result, release of paclitaxel occurs due to swelling for up to 24 h (Fig. 3). After 1 day, enzymes (e.g. lysozyme) that are present in solution cause degradation of the implant for up to 14 days in PBS lysozyme and in ascites fluid (Fig. 4). The enzymes that enter pores cause an increase in pore size and create connectivity between pre-existing pores. As seen in the SEM micrographs (Fig. 5), the average size of the pores increased with each subsequent week. This leads to an increase in surface area and results in an accelerated drug release. After 14 days, macromolecular relaxation becomes dominant within the matrix. Dang et al. observed the release of carmustine from the Gliadel[®] implant through pores created by polymer erosion [40]. Also, Lemaire et al. proposed a release model for biodegradable porous matrices, whose mechanism was governed by the dual action of diffusion and erosion. The drug release rate was greatly dependent on erosion rate, diffusion coefficient of the drug in the wetted polymer matrix, pore length and size [41]. Gaining an understanding of

the drug release mechanism provides a means to tailor the release profile. For example, in the case of the chitosan-ePC system the recognized influence of swelling and degradation of chitosan on drug release suggests that an increase in the lipid content would decrease the drug release rate [16].

3.7. In vivo release of paclitaxel from implant and biodistribution of paclitaxel from implant in plasma and tissues from Balb/c mice

To confirm our *in vitro* release results, the release profile of the drug was also assessed *in vivo* in healthy Balb/c mice. The implant provided a release of 20 mg/kg/day (which corresponds to a release rate of 3.3% per day). This result is comparable ($p > 0.05$) to our previously obtained *in vivo* results (5.4% drug released per day) [15]. Also, the *in vivo* release rate correlated well with the *in vitro* release rate in PBS lysozyme ($r^2 = 0.965$). As shown, in Figs. 6a and 6b relatively constant plasma and tissue levels of drug were observed up to four weeks indicating a constant *in vivo* release of paclitaxel from the implants. An average of $0.078 \pm 0.01 \mu\text{g/mL}$ of paclitaxel was detected in plasma at each time point over the four week study. Of note, this represents a serum concentration which exceeds the minimum effective concentration for paclitaxel ($0.043 \mu\text{g/mL}$) [42]. Also, the average concentration of paclitaxel in the plasma is also less than the concentration of the drug that has been shown to cause myelosuppression (e.g. $0.085 \mu\text{g/mL}$) [43].

Constant release was also indicated by the biodistribution of paclitaxel in liver, heart, kidney and small intestine as shown in Fig. 6b. The concentration of paclitaxel was found to be significantly higher ($p < 0.05$) in the liver, kidney and heart in comparison to the small intestine. Innocenti et al. showed that the highest concentration of paclitaxel was found in the liver of female Swiss mice after IP administration [44]. Similarly, the highest concentrations of paclitaxel administered in a variety of different formulations (e.g. chitosan film, liposomes and poloxamer

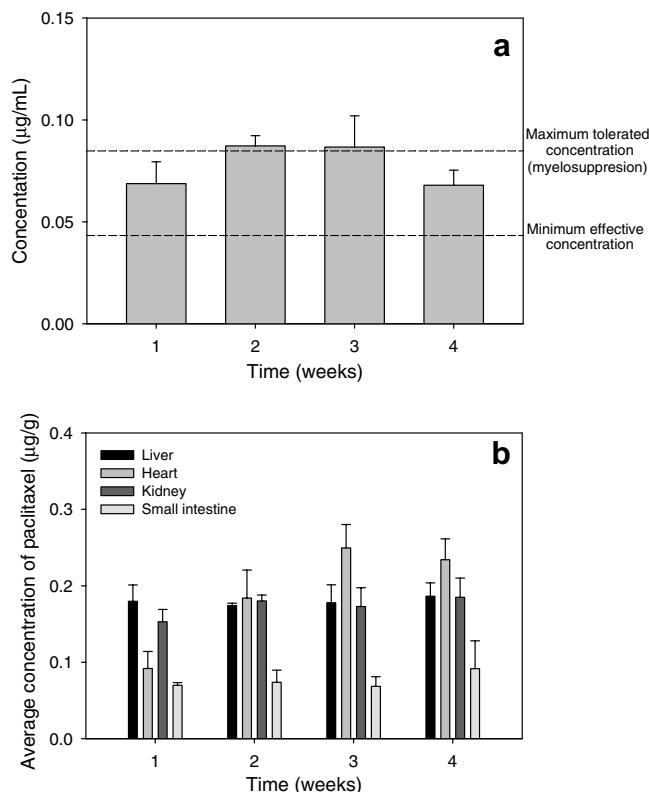


Fig. 6. (a) *In vivo* plasma concentrations and (b) *in vivo* biodistribution of PTX in various tissues (liver, kidney, heart and small intestine) of Balb/c mice ($n = 3$) implanted with a chitosan–ePC implant for periods of up to 4 weeks. Error bars are expressed as standard error ($n = 3$).

407 gel) were found in either the liver or kidney of mice [45]. Interestingly, we observed a slight increase of paclitaxel accumulation in the heart of mice implanted with the paclitaxel chitosan–ePC implant after 4 weeks. Accumulation in cardiac tissue is not altogether surprising as cardiac effects (such as asymptomatic bradycardia) have been previously reported in clinical studies with Taxol® [46].

4. Conclusions

The chitosan–ePC implant released paclitaxel *in vitro*, at a rate of approximately 1% per day, for up to 3 months in various physiologically relevant solutions (PBS lysozyme and ascites fluid). The release of paclitaxel in PBS lysozyme was well correlated with the release in ascites. Data obtained on the chitosan–ePC system were taken together to put forth a mechanism for the release of paclitaxel from this system that included swelling followed by degradation and then macromolecular relaxation as the dominant processes. The sustained release profile *in vitro* was confirmed *in vivo* following IP implantation of the chitosan–ePC system in Balb/c mice. In addition to the local exposure of paclitaxel to the peritoneal cavity, the implant was also found to result in a relatively low constant plasma concentration of drug over a four-week period.

Acknowledgements

The authors thank Mr. Ji Zhang for HPLC work done on the *in vivo* samples and Ms. Helen Lee for statistical analysis of the data. The project was funded by the Ontario Cancer Research Network (OCRN), the Natural Sciences and Engineering Research Council (NSERC) and the Canadian Cancer Society (CCS). Dr. Lim Soo is the recipient of a Canadian Institutes of Health Research (CIHR)-RX&D Health Research Foundation Fellowship.

References

- [1] Cancer Statistics 2006, Cancer Statistics 2006, American Cancer Society, Inc.
- [2] Cancer Facts and Figures 2006. Cancer Facts and Figures 2006, American Cancer Society Inc.
- [3] L. Elit, T.K. Oliver, A. Covens, J. Kwon, M.-K. Fung, H.W. Hirte, A.M. Oza, Intraperitoneal chemotherapy in the first-line treatment of women with stage III epithelial ovarian cancer: a systematic review with metaanalyses, *Cancer* 109 (4) (2007) 692–702.
- [4] S.A. Cannistra, Cancer of the ovary, *New England Journal of Medicine* 351 (24) (2004) 2519–2529.
- [5] NCI Issues Clinical Announcement for Preferred Method of Treatment for Advanced Ovarian Cancer. National Cancer Institute: <http://www.cancer.gov>.
- [6] D.K. Armstrong, B. Bundy, L. Wenzel, H.Q. Huang, R. Baergen, S. Lele, L.J. Copeland, J.L. Walker, R.A. Burger, Intraperitoneal cisplatin and paclitaxel in ovarian cancer, *New England Journal of Medicine* 354 (1) (2006) 34–43.
- [7] C.A. Hamilton, J.S. Berek, Intraperitoneal chemotherapy for ovarian cancer, *Current Opinion in Oncology* 18 (5) (2006) 507–515.
- [8] E.K. Rowinsky, R.C. Donehower, Paclitaxel (taxol), *New England Journal of Medicine* 332 (15) (1995) 1004–1014.
- [9] E. Harper, W. Dang, R.G. Lapidus, R.I. Garver Jr., Enhanced efficacy of a novel controlled release paclitaxel formulation (PAC-LIMER delivery system) for local-regional therapy of lung cancer tumor nodules in mice, *Clinical Cancer Research* 5 (12) (1999) 4242–4248.
- [10] S. Nsereko, M. Amiji, Localized delivery of paclitaxel in solid tumors from biodegradable chitin microparticle formulations, *Biomaterials* 23 (13) (2002) 2723–2731.
- [11] J.K. Jackson, X. Zhang, S. Llewellyn, W.L. Hunter, H.M. Burt, The characterization of novel polymeric paste formulations for intratumoral delivery, *International Journal of Pharmaceutics* 270 (1–2) (2004) 185–198.
- [12] S.J. Vukelja, S.P. Anthony, J.C. Arseneau, B.S. Berman, C. Casey Cunningham, J.J. Nemunaitis, W.E. Samlowski, K.D. Fowers, Phase I study of escalating-dose OncoGel® (ReGel®/paclitaxel) depot injection, a controlled-release formulation of paclitaxel, for local management of superficial solid tumor lesions, *Anti-Cancer Drugs* 18 (3) (2007) 283–289.
- [13] S.V. Fulzele, P.M. Satturwar, A.K. Dorle, Study of the biodegradation and *in vivo* biocompatibility of novel biomaterials, *European Journal of Pharmaceutical Sciences* 20 (1) (2003) 53–61.
- [14] A.C.R. Grayson, G. Voskerician, A. Lynn, J.M. Anderson, M.J. Cima, R. Langer, Differential degradation rates *in vivo* and *in vitro* of biocompatible poly(lactic acid) and poly(glycolic acid) homo- and co-polymers for polymeric drug-delivery microchip, *Journal of Biomaterials Science, Polymer Edition* 15 (10) (2004) 1281–1304.
- [15] E.A. Ho, V. Vassileva, C. Allen, M. Piquette-Miller, *In vitro* and *in vivo* characterization of a novel biocompatible polymer–lipid implant system for the sustained delivery of paclitaxel, *Journal of Controlled Release* 104 (1) (2005) 181–191.

- [16] J. Grant, M. Blicher, M. Piquette-Miller, C. Allen, Hybrid films from blends of chitosan and egg phosphatidylcholine for localized delivery of paclitaxel, *Journal of Pharmaceutical Sciences* 94 (7) (2005) 1512–1527.
- [17] E.A. Ho, P. Lim Soo, C. Allen, M. Piquette-Miller, Impact of intraperitoneal, sustained delivery of paclitaxel on the expression of P-glycoprotein in ovarian tumors, *Journal of Controlled Release* 117 (1) (2007) 20–27.
- [18] J. Grant, J.P. Tomba, H. Lee, C. Allen, Relationship between composition and properties for stable chitosan films containing lipid microdomains, *Journal of Applied Polymer Science* 103 (6) (2007) 3453–3460.
- [19] V. Vassileva, J. Grant, R. De Souza, C. Allen, M. Piquette-Miller, Novel biocompatible intraperitoneal drug delivery system increases tolerability and therapeutic efficacy of paclitaxel in a human ovarian cancer xenograft model, *Cancer Chemotherapy and Pharmacology* 60 (2007) 907–914.
- [20] S.L. Parsons, S.A. Watson, R.J.C. Steele, Malignant ascites, *British Journal of Surgery* 83 (1) (1996) 6–14.
- [21] R.A. Adam, Y.G. Adam, Malignant ascites: Past, present, and future, *Journal of the American College of Surgeons* 198 (6) (2004) 999–1011.
- [22] D. Quintanar-Guerrero, E. Allemann, H. Fessi, E. Doelker, Preparation techniques and mechanisms of formation of biodegradable nanoparticles from preformed polymers, *Drug Development and Industrial Pharmacy* 24 (12) (1998) 1113–1128.
- [23] EnzChek(R) Lysozyme Assay Kit (E-22013). EnzChek(R) Lysozyme Assay Kit manual, Molecular Probes Inc., USA, 2001, p. 3.
- [24] Bio Rad Protein Assay Technical Manual. Bio Rad Protein Assay Technical Manual, Bio-Rad Laboratories, USA, p. 25.
- [25] C. Peniche, W. Arguelles-Monal, N. Davidenko, R. Sastre, A. Gallardo, J. San Roman, Self-curing membranes of chitosan/PAA IPNs obtained by radical polymerization: preparation, characterization and interpolymer complexation, *Biomaterials* 20 (20) (1999) 1869–1878.
- [26] A.T. Metters, C.N. Bowman, K.S. Anseth, A statistical kinetic model for the bulk degradation of PLA-b-PEG-b-PLA hydrogel networks, *Journal of Physical Chemistry B* 104 (30) (2000) 7043–7049.
- [27] H.-F. Liang, C.-T. Chen, S.-C. Chen, A.R. Kulkarni, Y.-L. Chiu, M.-C. Chen, H.-W. Sung, Paclitaxel-loaded poly(γ -glutamic acid)-poly(lactide) nanoparticles as a targeted drug delivery system for the treatment of liver cancer, *Biomaterials* 27 (9) (2006) 2051–2059.
- [28] S.-S. Feng, L. Mu, K.Y. Win, G. Huang, Nanoparticles of biodegradable polymers for clinical administration of paclitaxel, *Current Medicinal Chemistry* 11 (4) (2004) 413–424.
- [29] S.W. Kim, Y.H. Bae, T. Okano, Hydrogels: swelling, drug loading, and release, *Pharmaceutical Research* 9 (3) (1992) 283–290.
- [30] P.L. Ritger, N.A. Peppas, A simple equation for description of solute release I. Fickian and non-Fickian release from non-swelling devices in the form of slabs, spheres, cylinders or discs, *Journal of Controlled Release* 5 (1) (1987) 23–36.
- [31] D.Y. Arifin, L.Y. Lee, C.-H. Wang, Mathematical modeling and simulation of drug release from microspheres: implications to drug delivery systems, *Advanced Drug Delivery Reviews* 58 (12–13) (2006) 1274–1325.
- [32] N.A. Peppas, J.J. Sahlin, A simple equation for the description of solute release. III. Coupling of diffusion and relaxation, *International Journal of Pharmaceutics* 57 (2) (1989) 169–172.
- [33] T. Alfrey, E.F. Gurnee, W.G. Lloyd, Diffusion in glassy polymers, *Journal of Polymer Science. Part C: Polymer Symposia* 12 (1966) 249–261.
- [34] Y.-E. Fang, Q. Cheng, X.-B. Lu, Kinetics of in vitro drug release from chitosan/gelatin hybrid membranes, *Journal of Applied Polymer Science* 68 (11) (1998) 1751–1758.
- [35] X.Y. Xiong, K.C. Tam, L.H. Gan, Release kinetics of hydrophobic and hydrophilic model drugs from pluronic F127/poly(lactic acid) nanoparticles, *Journal of Controlled Release* 103 (1) (2005) 73–82.
- [36] J.M. Kisler, G.W. Stevens, A.J. O'Connor, Adsorption of proteins on mesoporous molecular sieves, *Materials Physics and Mechanics* 4 (2001) 89–93.
- [37] R.J. Nordtveit, K.M. Varum, O. Smidsrod, Degradation of fully water-soluble, partially *N*-acetylated chitosans with lysozyme, *Carbohydrate Polymers* 23 (4) (1994) 253–260.
- [38] K. Tomihata, Y. Ikada, In vitro and in vivo degradation of films of chitin and its deacetylated derivatives, *Biomaterials* 18 (7) (1997) 567–575.
- [39] R.A.A. Muzzarelli, Human enzymatic activities related to the therapeutic administration of chitin derivatives, *Cellular and Molecular Life Sciences* 53 (2) (1997) 131–140.
- [40] W. Dang, T. Daviau, H. Brem, Morphological characterization of polyanhydride biodegradable implant Gliadel during in vitro and in vivo erosion using scanning electron microscopy, *Pharmaceutical Research* 13 (5) (1996) 683–691.
- [41] V. Lemaire, J. Belair, P. Hildgen, Structural modeling of drug release from biodegradable porous matrices based on a combined diffusion/erosion process, *International Journal of Pharmaceutics* 258 (1–2) (2003) 95–107.
- [42] J.E. Liebmann, J.A. Cook, C. Lipschultz, D. Teague, J. Fisher, J.B. Mitchell, Cytotoxic studies of paclitaxel (Taxol®) in human tumour cell lines, *British Journal of Cancer* 68 (6) (1993) 1104–1109.
- [43] M. Kobayashi, K. Oba, J. Sakamoto, K. Kondo, N. Nagata, T. Okabayashi, T. Namikawa, K. Hanazaki, Pharmacokinetic study of weekly administration dose of paclitaxel in patients with advanced or recurrent gastric cancer in Japan, *Gastric Cancer* 10 (1) (2007) 52–57.
- [44] F. Innocenti, R. Danesi, A. Di Paolo, C. Agen, D. Nardini, G. Bocci, M. Del Tacca, Plasma and tissue disposition of paclitaxel (taxol) after intraperitoneal administration in mice, *Drug Metabolism and Disposition* 23 (7) (1995) 713–717.
- [45] A.B. Dhanikula, D.R. Singh, R. Panchagnula, In vivo pharmacokinetic and tissue distribution studies in mice of alternative formulations for local and systemic delivery of paclitaxel: gel, film, prodrug, liposomes and micelles, *Current Drug Delivery* 2 (2005) 35–44.
- [46] E.K. Rowinsky, W.P. McGuire, T. Guarnieri, J.S. Fisherman, M.C. Christian, R.C. Donehower, Cardiac disturbances during the administration of taxol, *Journal of Clinical Oncology* 9 (9) (1991) 1704–1712.